Physica B 407 (2012) 1232–1237

Contents lists available at SciVerse ScienceDirect

Physica B

journal homepage: www.elsevier.com/locate/physb

Structural and magnetic properties of Mg substituted NiCuZn Nano Ferrites

Ch. Sujatha [a,*], K. Venugopal Reddy [a], K. Sowri Babu [a], A. RamaChandra Reddy [a], K.H. Rao [b]

[a] Department of Physics, National Institute of Technology, Warangal-506004, A.P, India
[b] Department of Physics, Andhra University, Visakhapatnam-530003, A.P, India

ARTICLE INFO

Article history:
Received 24 November 2011
Received in revised form
17 January 2012
Accepted 18 January 2012
Available online 31 January 2012

Keywords:
Sol-gel method
Nano ferrite
Magneto crystalline anisotropy constant
Initial permeability

ABSTRACT

The present paper examines the effect of magnesium substitution on structural and magnetic properties of NiCuZn nano ferrites synthesised by sol-gel method. The prepared samples were characterised by using X-ray Diffraction (XRD), Fourier transform infrared spectroscopy (FT-IR), Field Emission Scanning Electron Microscopy (FE-SEM) and Vibration sample magnetometer (VSM) techniques. The phase identification, unit cell parameter and crystallite size was determined using XRD analysis. The lattice constant reduced with increasing Mg content. Room temperature saturation magnetisation and coercivity showed reverse trend with increasing Mg content. Curie temperature (T_c) obtained from the thermo magnetic curves increases with Mg concentration. The initial permeability (μ_i) decreased with increasing Mg content. This is due to reduced magnetisation, grain size and increased magneto-crystalline anisotropy constant. Simultaneously, there is an upward shift of domain wall relaxation frequency with increasing Mg content. Also the permeability is observed to be constant up to 30 MHz frequency range showing compositional stability and quality of the material. The prepared samples were suitable for applications in Multilayer Chip Inductors due to their invariable permeability up to 30 MHz frequency and high thermal stability along with low sintering temperature.

1. Introduction

Magnetic nanoparticles of mixed spinel ferrites have been the subject of current interest because of their interesting magnetic, electric, dielectric and optical properties, which are considerably different from that of their bulk counterparts [1]. These properties can be tailored for a specific device applications by choosing the proper type of cations and their distribution among tetrahedral (A) and octahedral (B) sites of the spinel lattice. In addition, the preparation conditions such as sintering temperature, sintering time and the method of preparation are the other important parameters in this regard [2]. Recently there is a growing interest on Mg based ferrites to use in microwave devices because of their high electrical resistivity and low dielectric losses [3]. Besides that they possess high Curie temperature, environmental stability, hard mechanical properties and they are available at low cost [4]. Moreover, MgO is a very stable oxide and avoids the formation of divalent iron and thereby increasing its resistivity [5].

Varalakshmi et al. [6] examined NiMgCuZn system for stress insensitive multilayer chip inductor applications (MLCIs). Roy et al. [7] investigated electromagnetic properties of Mg substituted NiCuZn ferrites suitable for MLCIs. Gabal et al. [5] studied the magnetic properties of $Ni_{0.5-x}Mg_xCu_{0.2}Zn_{0.3}Fe_2O_4$ ferrites prepared using egg white as binder cum gelling for applications in miniaturised multilayer chip inductors. Bharati et al. [8] reported that $Mg_{0.8-x}Cu_{0.2}Zn_xFe_2O_4$ ferrites prepared through sol-gel auto combustion method exhibiting improved electromagnetic properties with increasing Zn substitution.

There are reports on the compositions of the type $Mg_xZn_{1-x}Fe_2O_4$ present in the literature demonstrating good dielectric properties [9–11]. A. Hossain et al. studied $Ni_{0.50}Zn_{0.50-x}Mg_xFe_2O_4$ system and found that though both Mg and Zn are non magnetic, there is a great effect on magnetic properties of ferrites due to the substitution of Zn by Mg [3]. Murbe et al. [12] investigated $Mg_{0.201+x-y}Cu_yZn_{0.62-x}Fe_{1.98}O_{3.99}$ ferrite with $0 \le x \le 0.2$ and $0 \le y \le 0.3$ for obtaining low sintering temperature, high permeability and high thermal stability and to use them as Multilayer chip inductor materials as an alternate to the NiCuZn ferrite system. Thus, substitution of Mg in place of Zn has got some advantages namely improved thermal stability, enhanced operating frequency and increased electrical resistivity [3,11].

Very few literature related to the effect of magnesium substitution in place of Zn on electromagnetic properties of NiMgCuZn nano ferrites exists [3,6]. In this context the present paper deals with systematic study of effects of Mg substitution in place of Zn, particularly, on structural and magnetic properties of $Ni_{0.5}Cu_{0.05}Zn_{0.45-x}Mg_xFe_2O_4$ ferrites which are prepared through sol-gel method. Since both Mg and Zn are non magnetic ions thus

* Corresponding author. Tel.: +91 8702462560; fax: +91 8702459547.
E-mail address: sujatha.phys09@gmail.com (Ch. Sujatha).

0921-4526/$ - see front matter © 2012 Elsevier B.V. All rights reserved.
doi:10.1016/j.physb.2012.01.108

there is no complexity in magnetic ordering. Here we focussed, our attention, mainly to observe how the change in the dimension of the cation and their distributions, over the two sub lattices, of a spinel will influence the structural and magnetic properties of ferrites.

2. Experimental

$Ni_{0.5}Cu_{0.05}Mg_xZn_{0.45-x}Fe_2O_4$ (x=0.09, 0.18, 0.27, 0.36 and 0.45) nano ferrites have been processed through sol-gel method. Analytical grade nickel, zinc, copper, magnesium and ferric nitrates were weighed in stoichiometric proportions and made dissolved separately in deionised water. Thus obtained cationic solutions were mixed one into another and stirred continuously for one hour in order to improve homogeneity. To the resulting solution, precursor, polyvinyl alcohol (PVA) solution was added drop by drop under constant stirring and heating. The gelation continued step by step till a red gel type product was formed with the release of reddish brown gases at about 100 °C, leaving the fluffy mass in the reaction vessel which was annealed at 500 °C for 3 h to remove PVA. This powder was compacted in the shape of disc shaped pellets and toroids which were sintered at 950 °C for 1 hour with a heating rate of 5 °C/min using temperature controlled muffle furnace.

The phase identification, lattice constant and crystallite size of the sintered samples were characterised by X-ray diffraction using Inel X-ray diffractometer (XRG 3000) with Co-Kα radiation (1.78897 Å). Formation of pure spinel phase was also confirmed using Fourier Transform Infrared spectra (BRUKER OPTICS TENSOR 27) recorded in the wave number region 4000-400 cm^{-1} using KBr pellet method. The morphology and grain size distribution of nanoparticles having gold with palladium coated surfaces were investigated by field emission scanning electron microscope(FE-SEM) of make Carl Zeiss Ultra 55, operating at an accelerating high tension voltage of 17 kV with a working distance (WD) of 8.5 mm;while the elemental analysis was carried out using Energy Dispersive X-ray spectroscopy (EDAX).Room temperature magnetic parameters were determined using vibration sample magnetometer (EV-7 VSM) in an applied magnetic field of 20 kOe. Temperature variation of magnetisation, in an applied magnetic field of 100 Oe is obtained up to a temperature range of 520 °C using the same instrument. Permeability spectra in the frequency range 20 Hz–50 MHz was obtained using High frequency LCR metre (WAYNKERR 6500 P).

3. Results and discussion

The X-Ray Diffraction patterns of the sintered $Ni_{0.5}Cu_{0.05}Mg_xZn_{0.45-x}Fe_2O_4$ (x=0.09, 0.18, 0.27, 0.36, 0.45) ferrites are as shown in Fig. 1. The existence of (3 1 1) peak, centre around $2\theta \approx 41^\circ$ confirms the formation of cubic spinel structure. The highest intensity (3 1 1) peak position with Cu-Kα radiation for spinel ferrites were observed conventionally around 35° but it is shifted towards higher angle side due to Co-Kα radiation. The well resolved peaks in the XRD pattern clearly indicate polycrystalline nature of the ferrites.

It is observed that there is nominal change in peak positions for all the compositions studied, indicating that, all the samples are crystallised in the same spinel phase with space group Fd3m [13]. The mean crystallite size is calculated from X-ray line broadening of the high intensity (3 1 1) diffraction peak using Debye Scherrer's equation

$$D_{xrd} = \frac{0.9*\lambda}{\beta \cos\theta}$$

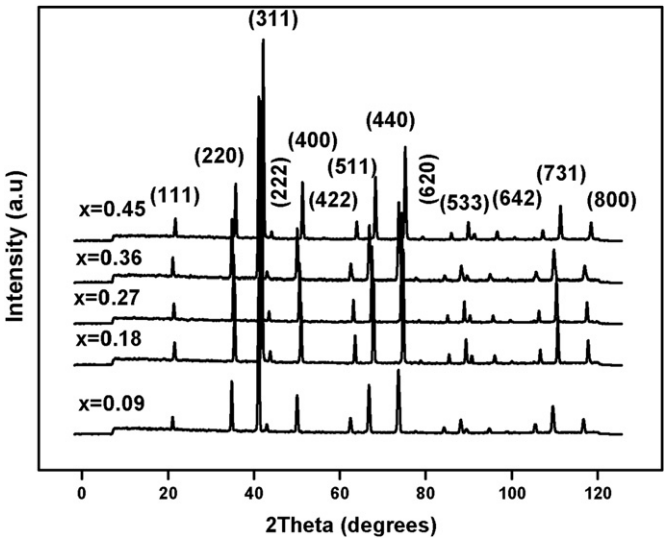

Fig. 1. XRD patterns of sintered $Ni_{0.5}Cu_{0.05}Mg_xZn_{0.45-x}Fe_2O_4$ ferrites for x=0.09, 0.18, 0.27, 0.36 and 0.45.

where λ is the wavelength of the X-rays (1.78897 Å), β is the full width at half maximum (in radians) and θ is the Bragg's angle.

Accurate estimation of lattice constant has been done using Nelson–Riley (NR) extrapolation method by minimising both systematic and random error. The values of the lattice parameter obtained from each reflected plane were plotted against the NR function $F(\theta)$ [14] and straight lines were obtained.

$$F(\theta) = \frac{1}{2}\left[\frac{cos^2\theta}{sin\theta} + \frac{cos^2\theta}{\theta}\right]$$

The extrapolation of these straight lines to $F(\theta)$=0 or θ=90° gives the accurate lattice constant. The lattice constant obtained from NR function showed decreasing trend with increasing magnesium content. This can be attributed to the smaller ionic size of Mg^{+2} (0.78 Å) substituted for Zn^{+2} (0.82 Å) [8].

The bulk density of the disc shaped pellet is calculated by considering mass and dimensions of the sample

$$d = \frac{mass}{volume}$$

$$d = \frac{m}{\prod r^2 * t}$$

where m is the mass and r, t are the radius and thickness of the pellet. The density decreased with magnesium substitution for zinc. This is due to magnesium having low atomic weight and density (24.305 amu, 1.738 g/cm^3) compared to zinc (65.39 amu, 7.14 g/cm^3). The lattice constant, crystallite size, density along with grain size and tetrahedral, octahedral frequency bands are as shown in Table 1.

IR spectroscopy is one of the useful tools to know the completion of the solid-state reaction; the cationic distribution; deformation in the spinel structure due to the entry of foreign ions [15]. The FTIR spectra (Fig. 2) showed only two prominent frequency bands around 400 and 600 cm^{-1} in the measured wave number range indicating that the samples are in pure spinel phase. In ferrite, the metal cations are situated according to the geometric configuration of the oxygen ion nearest neighbours, in two different sub lattices such as tetrahedral(A-sites) and octahedral sites (B-sites) [5]. The FT-IR spectra of the investigated ferrites showed two strong absorption bands in the wave number range 586–595 and 423–432 cm^{-1}. These bands (ν_1 and ν_2) are assigned to the vibrations of the metal-oxygen ion complexes in the tetrahedral and octahedral sites, respectively. This

Table 1
Lattice constant, bulk density, crystallite size, Grain size, Standard deviation in grain size, tetrahedral, and octahedral frequency bands of sintered $Ni_{0.5}Cu_{0.05}Mg_xZn_{0.45-x}Fe_2O4$ ferrites (x=0.09, 0.18, 0.27, 0.36 and 0.45).

x	0.09	0.18	0.27	0.36	0.45
Lattice constant a (Å)	8.38568	8.36385	8.37006	8.3825	8.33888
Density (g/cm^3)	3.60	3.56	3.40	3.14	3.07
Crystallite size D_{xrd} (nm)	37	49	60	39	47
Grain Size D (nm)	246	207	167	159	148
Standard deviation (nm)[a]	11	7	10	1	4
Tetrahedral band v_1(cm^{-1})	586	582	586	586	595
Octahedral band v_2(cm^{-1})	423	428	429	431	432

[a] Standard Deviation in measuring grain size from FE-SEM.

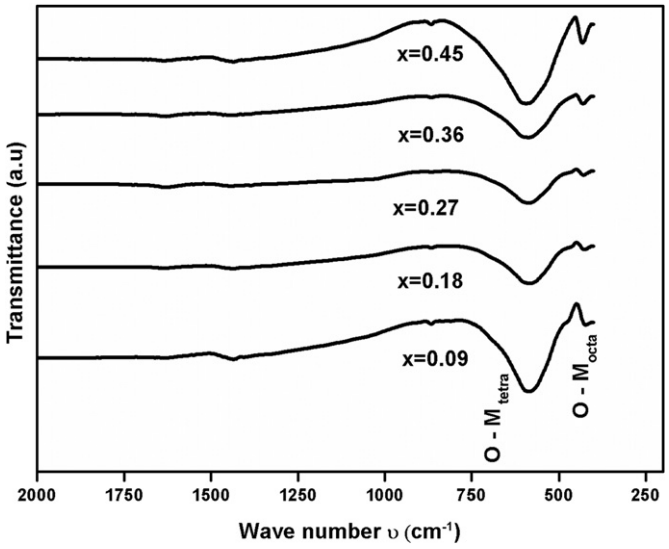

Fig. 2. FTIR spectra of sintered $Ni_{0.5}Cu_{0.05}Mg_xZn_{0.45-x}Fe_2O_4$ ferrites for x=0.09, 0.18, 0.27, 0.36 and 0.45.

difference in the band positions of v_1, v_2 is observed because of difference in the Fe^{3+}–O^{2-} distance for tetrahedral and octahedral complexes [16]. In general, these vibrational frequencies depend on cation mass, cation-oxygen distance and the bonding force [17]. The vibrational frequencies v_1, v_2 corresponding to tetrahedral and octahedral metal complexes are given in Table 1. It is observed that the frequency band v_2 shifts towards higher wave number side with increasing Mg concentration. This is due to Mg occupying octahedral sites with its larger ionic radius than Fe^{3+}(0.55 Å) ions, there by pushing Fe^{3+} ions towards oxygen ion resulting in reduced Fe^{3+}–O^{2-} bond length as there is an inverse relation between wave number and bond length. The values of v_1 remains constant with increase in Mg concentration up to x=0.36 and increases thereafter. The increase in frequency bands (v_1 and v_2) are also in good agreement with the reduced unit cell dimensions [18]. It is noticed that the absorption peaks are broadened with Mg substitution which implies that the structure is inverse spinel [17]. This is due to statistical distribution of Fe^{3+} ions in A and B -sites based on stoichiometric composition.

The magnetic properties of a material are sensitive to its microstructure. Fig. 3 shows Field Emission Scanning Electron Microscope (FE-SEM) micrographs for the sintered samples $Ni_{0.5}Cu_{0.05}Zn_{0.45-x}Mg_xFe_2O_4$ with x=0.09, 0.18, 0.27, 0.36 and 0.45. With increasing magnesium content, the nature of microstructure gets modulated. The chemical composition of the samples were also analysed by energy-dispersive X-ray spectroscopy (EDAX). The calculated weight percentage of Ni/Cu/Zn/Mg/Fe values matches well with the amount of Ni/Cu/Zn/Mg/Fe used in the respective precursors. Thus EDAX analysis confirms that magnesium enters in to lattice and there is no segregation of impurity phase at the grain boundary. This implies complete solid solubility of magnesium in the present samples. The grain size of the samples with standard deviation was obtained by counting a sufficiently large number of grains to ensure accuracy. The grain size(D) declines with increasing magnesium concentration. The average grain sizes of all the samples are 246 nm, 207 nm, 167 nm, 159 nm and 148 nm, respectively indicating decrease in D. The grain size for the present samples is higher than the observed crystallite size (D_{xrd}) obtained from XRD using Debye Scherrer's equation. This can be realized that grains are formed by aggregation of small crystallites. The decreasing trend in grain size was also observed in compositions like $Ni_{0.5}Mg_xZn_{0.5-x}Fe_2O_4$ bulk ferrites, $Mg_xZn_{1-x}Fe_2O_4$ nano ferrites similar to the present samples [3,19]. This is because MgO acts as a microstructural stabilizator responsible for finer and uniform grain sizes [20]. Also MgO is a stable oxide avoids presence of divalent iron and there by circumvent tendency of discontinuous grain growth [5].

Room temperature hysteresis loops of Mg substituted NiCuZn ferrites (Fig. 4) indicate the soft ferrimagnetic nature in all the samples. The magnetic parameters such as saturation magnetisation (M_s), remanent magnetisation (M_r) and coercivity (H_c) (Table 2.) were obtained from hysteresis loop (M-H loop) and these parameters showed dependence on both composition and microstructure. Saturation magnetisation (M_s) decreases with increasing Mg content. These variations in magnetisation can be explained on the basis of super- exchange interactions among A and B sites in the spinel lattice. In general, in bulk ferrites, Zn^{2+} ions tend to occupy A-sites, Ni^{2+} have preference to occupy B-sites and Mg^{2+} ions have their strong preference for B-sites and a very few have preference to occupy A-sites, whereas Cu^{2+} and Fe^{3+} have usual preference for both the sites [5]. The preference of Mg^{2+} ions in to the B- site will encourage migration of Fe^{3+} ion in to A-site causing increasing magnetisation of A-site while that of B-site magnetisation decreases. Thus there is a net magnetisation, M_B-M_A, decrease with increasing magnesium content. Also reduced grain size (D) with magnesium content, results in increased number of grain boundaries may be the other reason for reduced magnetisation.

In general, the magnetic coercivity of a polycrystalline ferrite depends on magneto crystalline anisotropy constant (K_1) and grain size (D). Coercivity (H_c) increases with increasing Mg content this is because of two reasons. The first reason is reduced grain size with magnesium [20]. The second reason for the enhancement of coercivity is due to increased magneto crystalline anisotropy. Inverse relation between grain size and coercivity is clearly observed in the present samples and is shown in Fig. 5. Dinesh Varshney et al. [13] studied the $AxCo1_{-x}Fe_2O_4$ (A=Zn or Mg) system and the results showed that the coercivity tends to decrease with the substitution of either Mg or Zn. But with Mg substitution, the reduction of coercivty is less compared to Zn in the same $CoFe_2O_4$ host. There are few reports suggesting that with magnesium substitution for Zn, improves coercivity [6,21]. This is due to high magneto crystalline anisotropy constant (K_1) of Mg over Zn as coercivity has linear relationship with magneto crystalline anisotropy constant (K_1). Increased magneto crystalline anisotropy constant can be realized with the following explanation. It is known that magneto crystalline anisotropy constant depends on atomic coordination and thus it changes in A and B sites [22]. Magnesium occupying octahedral sites substituted for zinc(A site) may have partial contribution of orbital moment unquenched by crystal field which causes improvement of spin orbit interaction and there by anisotropy constant increases [23].

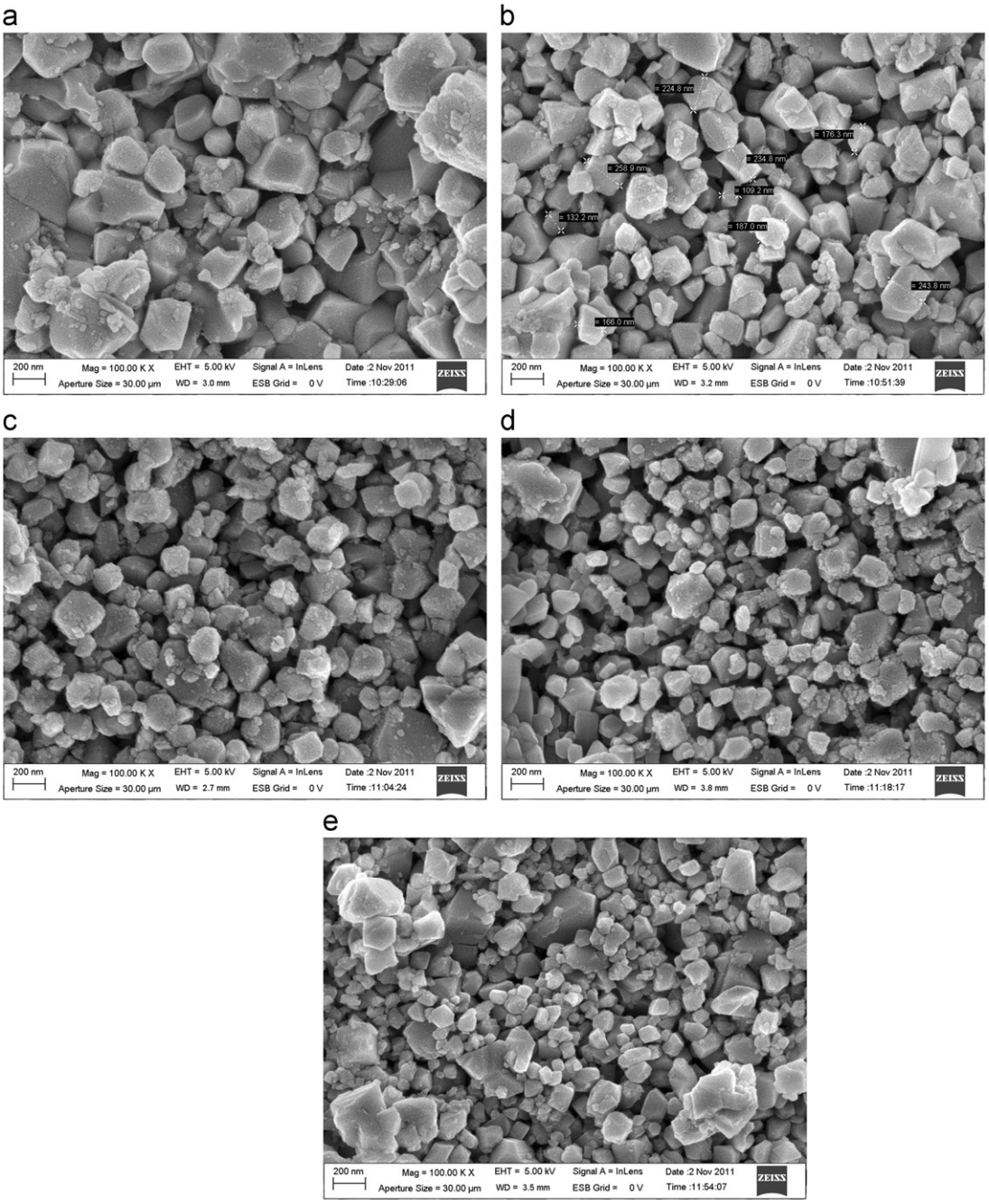

Fig. 3. Micrographs of sintered $Ni_{0.5}Cu_{0.05}Mg_xZn_{0.45-x}Fe_2O_4$ ferrites for (a) $x=0.09$, (b) 0.18, (c) 0.27, (d) 0.36 and (e) 0.45.

Fig. 6 shows thermo magnetic curves for the $Ni_{0.5}Cu_{0.05}Mg_xZn_{0.45x}Fe_2O_4$($x=0.09$, 0.18, 0.27, 0.36, 0.45) sintered samples in the static applied magnetic field of 100 Oe. According to Neel theory there are three types of exchange interactions (AA, BB, AB) exist in the ferrite material and out of which AB exchange interaction is predominant. These exchange interactions are responsible for ordered alignment of spins in A and B sites in ferrites. Curie temperature (T_c) of the ferrite material provides an idea about the amount of thermal energy required to disrupt these exchange interactions and it can be determined from magnetic moment versus temperature curves. The samples exhibit ferrimagnetic behaviour before reaching the Curie temperature T_c, after that the paramagnetic nature dominates. The compositional variation of Curie temperature T_c showed increasing trend with increasing Mg concentration (Table 2). This is due to Mg substituted for Zn occupies B sites, displacing Fe^{3+} ions to A sites resulting in increased number of ferromagnetic iron ions (Fe^{3+}) as the neighbours to B site ion ensuing increased AB exchange interaction. Besides that, the reduced unit cell dimension (a) with increased Mg content improves exchange interactions between the magnetic ions [24]. This is another factor contributes to the increase of Curie temperature as a function of Mg composition. Thus improvement in AB exchange interaction with Mg substitution for Zn require greater amount of thermal energy for offsetting the spin alignment. These samples exhibited good thermal stability up to a temperature of 500 °C, which is one of the requirements for Multilayer Chip Inductor (MLCIs) materials. Curie temperature for the bulk

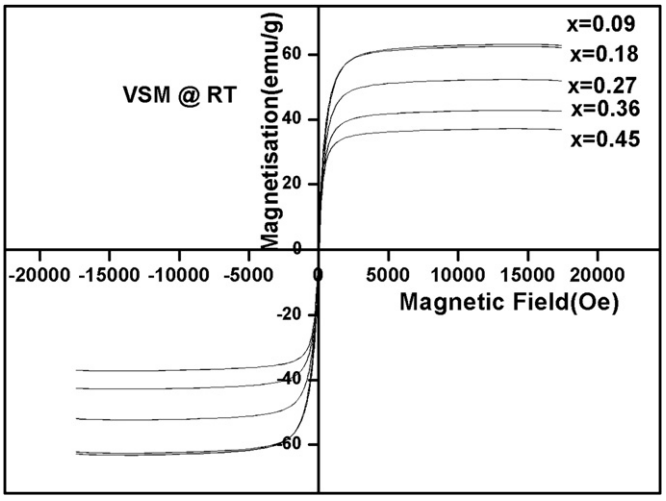

Fig. 4. Room temperature Hysteresis loops of sintered $Ni_{0.5}Cu_{0.05}Mg_xZn_{0.45-x}Fe_2O_4$ ferrites for $x=0.09$, 0.18, 0.27, 0.36 and 0.45.

Table 2
Saturation magnetisation, coercivity, remanent magnetisation, Curie temperature, initial permeability, Domain wall relaxation frequency and quality factor of sintered $Ni_{0.5}Cu_{0.05}Mg_xZn_{0.45-x}Fe_2O4$ ferrites for $x=0.09$, 0.18, 0.27, 0.36 and 0.45.

x	0.09	0.18	0.27	0.36	0.45
Saturation Magnetisation M_s (emu/g)	63.23	62.61	52.36	42.83	37.18
Coercivity H_c(Oe)	26	24.62	38.05	53.72	56.35
Remnant Magnetisation M_r (emu/g)	3.064	3.66	4.645	6.058	6.502
Curie Temperature T_c (°C)	380	404	438	501	514
Initial Permeability μ_i'at 1 MHz	56	29	24	23	15
Domain wall relaxation frequency f_r (MHz)	30	30.5	32.5	34	35
Quality factor Q at 1 MHz	54.8	40.2	39	26.2	19.9

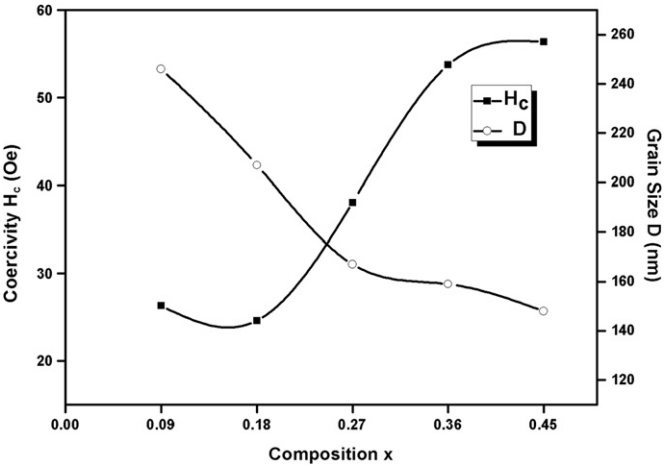

Fig. 5. Variation of coercivity and grain size with composition for $Ni_{0.5}Cu_{0.05}Mg_xZn_{0.45-x}Fe_2O_4$ ferrites with $x=0.09$, 0.18, 0.27, 0.36 and 0.45.

$Ni_{0.5}Zn_{0.5-x}Mg_xFe_2O_4$ samples varies from 236 to 487 °C with Mg content [3]. In the present case, even for the lowest Mg composition ($x=0.09$), the sample has T_c at about 380 °C which increases further with increase of Mg concentration. These T_c values are reasonably high compared to the similar type of compositions exist in the literature [3,6,12].

Fig. 7 shows frequency dispersion of permeability spectra for magnesium substituted NiCuZn nano ferrites up to 50 MHz frequency range at room temperature conditions. In general,

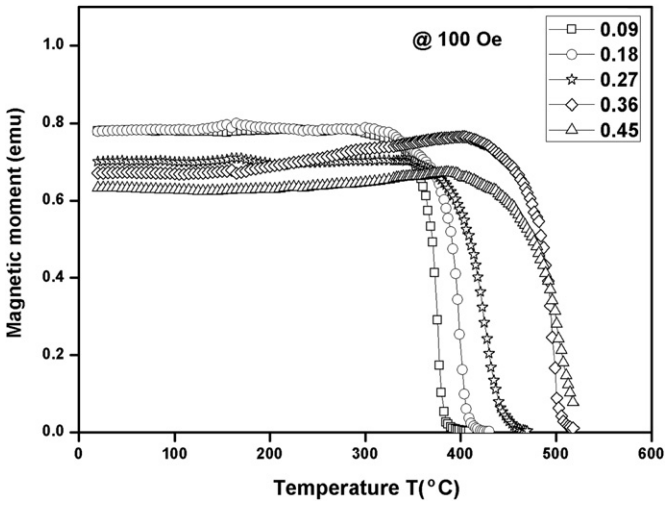

Fig. 6. Thermo magnetic curves of $Ni_{0.5}Cu_{0.05}Mg_xZn_{0.45-x}Fe_2O_4$ ferrites for $x=0.09$, 0.18, 0.27, 0.36 and 0.45.

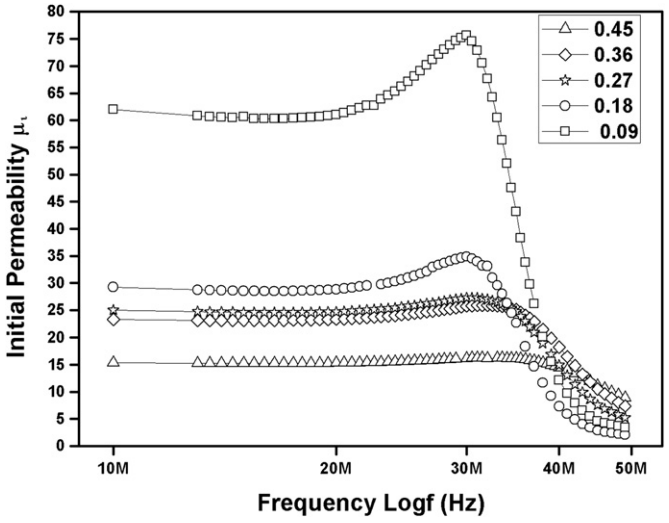

Fig. 7. Initial permeability versus frequency for sintered $Ni_{0.5}Cu_{0.05}Mg_xZn_{0.45-x}Fe_2O_4$ ferrites for $x=0.09$, 0.18, 0.27, 0.36 and 0.45.

permeability of a polycrystalline ferrite is related to two different magnetisation mechanisms; spin rotational and domain wall magnetisations [25]. At lower frequencies domain wall motion has major contribution to the permeability than spin rotation. The permeability due to domain wall motion is given by [8]

$$(\mu_i)_{dw}\alpha\frac{M_s^2 D}{K_1}$$

where M_s is the saturation magnetisation, D is the average grain size, and K_1 is the magneto crystalline anisotropy constant. As the domain wall motion is greatly influenced by the grain size, its contribution to the permeability is enhanced with increasing grain size. The initial permeability, showed flat profile with frequency up to 30 MHz indicating compositional stability and quality of the material. The constancy of permeability with applied ac frequency is called zone of utility of the material and it is about 30 MHz for the present samples. The variation of permeability with composition (Table 2.) decreases with increasing magnesium content. This can be explained by considering variations of magnetisation, grain size and anisotropy constant with increased magnesium substitution. As discussed earlier,

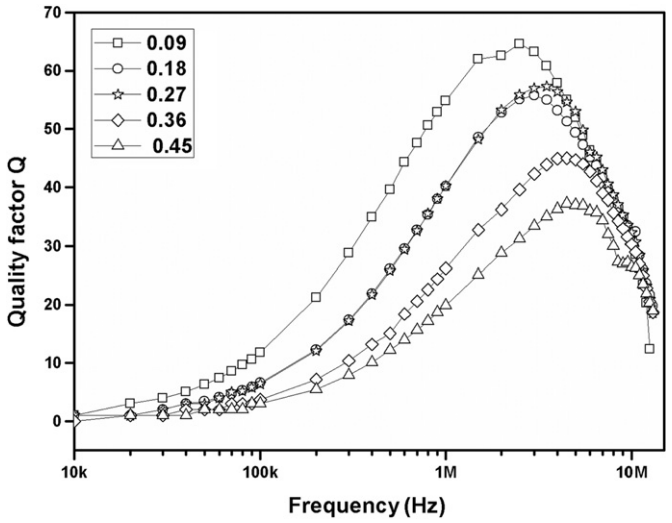

Fig. 8. Quality factor versus applied frequency for sintered $Ni_{0.5}Cu_{0.05}Mg_xZn_{0.45-x}Fe_2O_4$ ferrites for $x=0.09$, 0.18, 0.27, 0.36 and 0.45.

saturation magnetisation showed decreasing trend; while the microstructure exhibited increased homogeneity with finer grains; at the same time, there is an improved magneto crystalline anisotropy constant, with the increase of magnesium concentration. All these parameters put together, adversely affect the permeability, causing to decrease its value with increasing magnesium substitution. Static initial permeability (μ_i') at 1 MHz frequency showed decreasing trend with increasing Mg substitution starting from 56 to 15 (Table 2). There are reports supporting that ferrites prepared through chemical route methods showed similar orders of permeability values as that of observed results [19,26]. The obtained permeability values are lower than the reported bulk ferrites but showing similar behaviour [3,6]. These differences are due to the method of preparation, sintering temperature and time. The present samples were sintered at 950 °C (grain size (D) <0.5 μm) which is lower than sintering temperatures required in conventional ceramic methods (≈ 1250 °C grain size(D) ≥ 2 μm). The magnetic properties like permeability are known to be influenced by extrinsic parameters (like grain size (D), density(d) etc.); this may be the reason for lower values of permeability compared to the reported results [3,6]. MLCI materials are required to be sintered at a temperature <961 °C (Melting point of silver electrode) in order to avoid diffusion of silver in to the ferrite materials; which will deteriorate material properties. Thus, the present samples are suitable for MLCIs applications. Further, domain wall relaxation frequency (f_r) shifts towards higher frequency side from 30 MHz to 35 MHz with Mg composition (Table 2). Thus, the samples exhibiting high frequency stability within the frequency band from 1 MHz to 30 MHz. The decrease in permeability and increase in relaxation frequency are in good agreement with the Snoek's law.

The Quality factor (Q) of the material increases with increase in frequency showing (Fig. 8) a peak and there after decreases at higher frequencies, due to ferrimagnetic resonance (FMR) losses. These losses are mainly due to phase lag of domain wall motion with respect to the applied ac magnetic field. The Quality factor showed decreasing trend with increasing magnesium content; this is due to increased number of defects (like increased number of grain boundaries) with the magnesium substitution. The peak corresponding to maximum of Q-factor shifts towards higher frequency range as magnesium content increases.

4. Conclusions

$Ni_{0.5}Cu_{0.05}Mg_xZn_{0.45-x}Fe_2O_4$ nano ferrites prepared through sol-gel method showed single phase spinel structure with no secondary phases. The saturation magnetisation and grain size decreased with increasing Mg content whereas coercivity increased. The Initial permeability was reduced with composition but remains constant with frequency up to 30 MHz. Improvement in Curie temperature with Mg composition provides good thermal stability. Both the domain wall relaxation frequency and quality factor shifted towards higher frequency side with the substitution of magnesium. It is observed that the structural and magnetic properties are greatly changed with the substitution of Mg for Zn. The samples having constant permeability up to 30 MHz frequency and low sintering temperature can find applications in multilayer chip inductors.

Acknowledgements

The authors are grateful to Prof. C. Bansal, Dean, School of Physics, University of Hyderabad for generously providing XRD and FE-SEM facilities. Also, the authors would like to express thanks to Dr. G. Jagan Reddy and Dr. A.R. James, DMRL, Hyderabad; Dr. P. Sarah, Vardaman Engineering college Hyderabad for providing magnetic measurements.

References

[1] P.K. Chakrabarti, B.K. Nath, S. Brahma, S. Das, K. Goswami, U. Kumar, P. Mukhopadhyay, D. Das, M. Ammar, F. Mazaleyrat, J. Phys.: Condens. Matter 18 (2006) 5253.
[2] M. Anis-ur-Rehman, Muhammad Ali Malik, M. Akram, Kishwar Khan, Asghari Maqsood, Phys. Scr. 83 (2011) 015602. (6pp).
[3] K.M. AktherHossain, T.S. Biswas, Takeshi Yanagida, Hidekazu Tanaka, Hitoshi Tabata, Tomoji Kawai, Mater. Chem. Phys. 120 (2010) 461.
[4] Xiwei Qi, Ji Zhou, Zhenxing Yue, Zhilun Gui, Longtu Li, J. Magn. Magn. Mater. 251 (2002) 316.
[5] M.A. Gabal, J. Magn. Magn. Mater. 321 (2009) 3144.
[6] Narla Varalaxmi, N. Ramamanohar Reddy, Mudinepalli VenkataRamana, Eyunni Rajagopal, V. Ramakrishna Murthy, Kota Venkata Sivakumar, J Mater Sci: Mater. Electron. 19 (2008) 399.
[7] P.K. Roy, J. Bera, J. Magn. Magn. Mater. 298 (2006) 38.
[8] M.R. Barati, J. Alloys. Compd. 478 (2009) 375.
[9] S. Ghatak, M. Sinha, A.K. Meikap, S.K. Pradhan, Physica E 42 (2010) 1397.
[10] M.H. Abdullah, A.N. Yusoff, J. Mater. Sci. 5 (1997) 815.
[11] M.A. El Hiti, J. Magn. Magn. Mater. 192 (1999) 305.
[12] Julia Murbe, Jorg Topfer, Int. J. Appl. Ceram. Technol. (2007) 4154[5] (2007) 415.
[13] Dinesh Varshney, Kavita Verma, Ashwini Kumar, J. Mol. Struct. Article in press (2011) 447.
[14] M. Manjurul Haque, M. Huq, M.A. Hakim, J. Phys. D Appl. Phys. 41 (2008) 055007. (10pp).
[15] Hussein A. Dawoud, Samy K. Shaat, H. Dawoud, J. Al-Aqsa Unv. 10 (S.E) (2006) 247.
[16] B.K. Labde, Madan C. Sable, N.R. Shamkwar, Mater. Lett. 57 (2003) 1651.
[17] S.A. Patil, V.C. Mahajan, A.K. Ghatage, S.D. Lotke, Mater. Chem. Phys. 57 (1998) 86.
[18] Navneet Singh, Ashish Agarwal, Sujata Sanghi, Paramjeet Singh, Physica B 406 (2011) 687.
[19] A. Daigle, J. Modest, A.L. Geiler, S. Gillette, Y. Chen, M. Geiler, B. Hu, S. Kim, K. Stopher, C. Vittoria, V.G. Harris, Nanotechnology 22 (2011) 305708. (6pp).
[20] E. Rezlescu, N. Rezlescu, P.D. Popa, L. Rezlescu, C. Pasnicu, M.L. Craus, Mater. Res. Bull. 33 (6) (1998) 915.
[21] B.K. Nath, P.K. Chakrabarti, S. Das, U. Kumar, P.K. Mukhopadhyay, D. Das, J. Surface Sci. Technol. 21 (3–4) (2005) 169.
[22] Fausto Fiarillo, Measurement and characterization of magnetic materials, First ed., Elsevier Academic press, 2004, 71pp.
[23] B.D. Cullity, C.D. Graham, Introduction to magnetic materials, Second ed., Willey publishers, 2009, 102pp.
[24] A. Globus, H. Pascard, V. Cagan, J. Phys. c1 4 (1997) 163.
[25] T. Nakamura, J. Magn. Magn. Mater. 168 (1997) 285.
[26] Ningjie Chu, Xinqing Wang, Yapi Liu, Hongxiao Jin, Qiong Wu, Li Liang, Zisheng Wang, Hongliang Ge, J. Alloys. Compd. 470 (2009) 438.